A Gas- and Condensed-Phase Density Functional Study of Donor−Acceptor Complexes of Sulfur Trioxide

Brian N. Ida, Peter S. Fudacz, Douglas H. Pulsifer, and Jean M. Standard*

Department of Chemistry, Illinois State University, Normal, Illinois 61790-4160

Received: August 15, 2005; In Final Form: November 23, 2005

A series of donor−acceptor complexes containing sulfur trioxide have been studied in the gas and condensed phases using density functional theory. The condensed phase is represented using the polarizable continuum model. The systems investigated include complexes of nitrogen-containing donor molecules, $(CH_3)_nH_{3-n}N$ ($n = 0-3$), with SO_3 and complexes of oxygen-containing donor molecules, $(CH_3)_mH_{2-m}O$ ($m = 0-2$), with SO_3. Significant differences are observed between the gas- and condensed-phase properties of the complexes as a result of the ability of the condensed-phase medium to support higher charge separation between the donor and acceptor. The gas/condensed-phase behavior of two nitrogen-containing complexes, $(CH_3)H_2N-SO_3$ and $(CH_3)_2HN-SO_3$, has been investigated for the first time. These complexes exhibit properties intermediate to the previously observed H_3N-SO_3 and $(CH_3)_3N-SO_3$ complexes. Systematic trends in the gas- and condensed-phase structure and properties have been observed as methyl groups are added to the donor molecule. In addition, two oxygen-containing complexes, CH_3OH-SO_3 and $(CH_3)_2O-SO_3$, have been characterized for the first time. The differences between the gas- and condensed-phase properties of the oxygen-containing complexes are, in many cases, larger than those of the nitrogen-containing complexes, and therefore they represent an intriguing new class of complexes for potential experimental observation. Finally, a strong correlation between the charge transfer and binding energy has been obtained for both the nitrogen- and oxygen-containing complexes of sulfur trioxide.

Introduction

A variety of donor−acceptor complexes have been shown experimentally to exhibit large differences between their gas-phase and solid-state structures.[1−13] In particular, a great deal of work has focused on complexes involving BF_3,[2−5] SO_2,[6−8] and SO_3.[9−13] The donor−acceptor bond distances in these complexes show substantial decreases of 0.07−0.84 Å in the solid state compared to the gas-phase values. The largest structural change to date, 0.84 Å, was observed for the HCN−BF_3 complex, which exhibits a B−N distance of 2.473 Å in the gas phase[4] compared to 1.638 Å in the solid state.[5] Donor−acceptor complexes formed between nitrogen-containing compounds and SO_2 or SO_3 show more modest structural changes in their gas and solid-phase structures. For example, the complex of trimethylamine (TMA) with SO_2 exhibits a decrease in the S−N distance of 0.21 Å in the solid phase compared to the gas phase, while, in the TMA−SO_3 complex, the decrease is only 0.07 Å.

The large variation in the donor−acceptor bond distance between the gas and solid phases is also accompanied by other structural and electronic changes, including changes in bond angles and dipole moments. For example, the F−B−N bond angle of HCN−BF_3 increases from 91.5° in the gas phase[4] to 105.6° in the solid phase,[5] while the O−S−N bond angle of H_3N-SO_3 increases by 4.9° between the gas phase and the solid state. The dipole moments of these donor−acceptor complexes in many cases show significant enhancements in the solid state relative to the gas phase. For example, the gas-phase dipole moment of H_3N-SO_3 has been determined to be 6.2 D[14] compared to the solid-state value of 9.6 D.[15]

Ab initio quantum mechanical methods have been employed by previous workers in an attempt to explain the large gas/solid structural and electronic differences found in the various donor−acceptor complexes discussed above.[16−21] In early work, Wong, Wiberg, and Frisch employed the self-consistent reactant field (SCRF) method at the Hartree−Fock level of theory to model the structure of the H_3N-SO_3 complex in the condensed phase.[16] The changes in structural and electronic properties observed between the condensed-phase SCRF results and computed gas-phase results showed qualitative agreement with the experimental observations. Energy decomposition analysis determined that electrostatic and charge-transfer terms were the main contributors to the interaction energy of the complex. The calculated charge transfer increased from 0.28 to 0.36 e from the gas phase to the condensed phase, and topological analysis indicated that the covalent character of the S−N bond increased in the condensed phase. Following the initial work of Wong et al., Cioslowski and Martinov carried out gas-phase and SCRF calculations at the HF/6-311++G(d,p) level on a variety of systems in the gas and condensed phases, including H_3N-SO_3.[17] For the H_3N-SO_3 complex, the authors used charge-constrained calculations to show that solvation led to the strengthening of both the charge transfer and the covalent components of the S−N bond.

Another early computational study by Frenking and co-workers focused on a variety of gas-phase donor−acceptor complexes and also discussed gas/condensed-phase differences in the structure and properties of H_3N-BH_3.[18] The condensed phase was simulated by optimizing the geometries of dimers and tetramers of H_3N-BH_3. At the MP2 level of theory, Frenking and co-workers found that the dipole−dipole interactions of the dimer and tetramer of H_3N-BH_3 accounted for

* Corresponding author. E-mail address: standard@ilstu.edu.

10.1021/jp0545905 CCC: $33.50
Published on Web 04/07/2006

about 60% of the B−N bond shortening observed in the experimental solid-state structure compared to that found in the gas-phase structure.

Two recent quantum mechanical studies have also focused on the gas- and condensed-phase properties of the H_3N-BH_3 complex.[19,20] In one study, dimers of the complex were studied by Vela and co-workers at the B3LYP/6-311++G(d,p) level of theory in order to probe the interactions responsible for gas-to-solid-phase variations in geometry and other properties.[19] In accord with the conclusions of Frenking and co-workers,[18] the authors found that dipole−dipole interactions were primarily responsible for the gas/solid differences. In another study, Dillen and Verhoeven employed a grid of up to 30 H_3N-BH_3 molecules with fixed coordinates surrounding a central H_3N-BH_3 molecule at the MP2/6-31G(d) level of theory in order to model the solid phase.[20] These workers observed a significant shortening of the B−N bond, even with their smallest model (eight H_3N-BH_3 molecules surrounding one central H_3N-BH_3 molecule) and thus concluded that short-range interactions were primarily responsible for the bond contraction. However, additional changes in the B−N distance were observed as the size of the model increased; therefore, it was concluded that long-range interactions had some impact upon the solid-state structure.

Another recent computational study by Choo et al. employed density functional theory and the SCRF solvation model to investigate gas/condensed-phase differences in the $TMA-SO_2$ and $TMA-SO_3$ complexes.[21] The results obtained were consistent with available experimental data and showed a smaller contraction of the S−N bond in condensed media for the $TMA-SO_3$ complex than for the $TMA-SO_2$ complex. Choo et al. also observed increases in dipole moments and charge transfer for the complexes upon solvation, in accord with previous experimental and computational observations.

In addition to their interesting properties in the gas and condensed phases, some of the donor−acceptor complexes of sulfur trioxide are atmospherically significant. In particular, the gas-phase H_2O-SO_3 complex is an important precursor in acid rain formation. The H_2O-SO_3 complex has been detected in matrix experiments,[22−24] its structure has been elucidated by microwave spectroscopy,[25] and it has been the subject of numerous computational studies.[26−34] The gas-phase H_3N-SO_3 complex also has been detected using microwave spectroscopy[9] and has been postulated to be a possible nucleation site for the formation of atmospheric aerosols.[35] A variety of computational studies have sought to characterize the H_3N-SO_3 complex in the gas phase,[16,36−38] and recent experimental and computational studies have also focused on the interactions of SO_3 with both NH_3 and H_2O present.[39−41]

While some computational work has been performed on gas- and condensed-phase donor−acceptor complexes of sulfur trioxide, there have been no systematic investigations of the gas- and condensed-phase properties of complexes formed between sulfur trioxide and amines. In this work, density functional methods along with the polarizable continuum model (PCM) for solvation will be employed in order to carry out a systematic study of the gas- and condensed-phase behavior of intermolecular complexes formed between SO_3 and ammonia, methylamine (MA), dimethylamine (DMA), and TMA. This series encompasses two compounds investigated experimentally in both the gas and condensed phases, H_3N-SO_3[9,10] and $TMA-SO_3$.[11,12] The other two complexes, $MA-SO_3$ and $DMA-SO_3$, have been characterized experimentally only in the solid state.[42,43] This set of donor−acceptor complexes provides an intriguing series for exploration because of the disparate gas/condensed-phase behavior as methyl groups are added to the donor molecule; for example, the H_3N-SO_3 complex exhibits a rather large gas/solid variation in properties, while the variation observed for $TMA-SO_3$ is much smaller. Furthermore, the gas- and condensed-phase behavior of intermolecular complexes formed between SO_3 and water, methanol, and dimethyl ether will be scrutinized. This series of complexes includes the H_2O-SO_3 compound studied previously in the gas phase. In addition, the properties of two new complexes never before probed by either experimental or computational methods, CH_3OH-SO_3 and $(CH_3)_2O-SO_3$, will be presented, and their interesting gas/condensed-phase behavior will be predicted for the first time.

Computational Methods

Full geometry optimizations and vibrational frequency calculations were performed for the intermolecular complexes $(CH_3)_nH_{3-n}N-SO_3$ ($n = 0-3$) and $(CH_3)_mH_{2-m}O-SO_3$ ($m = 0-2$), along with all the monomers. The Gaussian 98[44] and Gaussian 03[45] software packages were utilized for all computations. The calculations were performed using the B3LYP density functional method and standard 6-31+G(d) and 6-311++G(d,p) basis sets. For the condensed-phase calculations, the PCM as implemented in Gaussian was employed to account for continuum solvation effects. Choo et al. noted that the condensed-phase structures and properties are fairly insensitive to the choice of dielectric constant;[21] therefore, all calculations in this work were performed using a dielectric constant of 78 to represent a highly polar condensed-phase medium.

Binding energies of the intermolecular complexes were computed relative to the separated monomers and were corrected for vibrational zero-point energies. Choo et al. studied basis set superposition error (BSSE) effects for $TMA-SO_2$ and $TMA-SO_3$ and concluded that BSSE had some effect on the geometries of the $TMA-SO_2$ and $TMA-SO_3$ complexes.[21] These authors found that the inclusion of BSSE led to a contraction of the S−N bond distance of 0.04 Å for $TMA-SO_2$ and 0.12 Å for $TMA-SO_3$ at the MPW1PW91/6-311+G(3df) level of theory. This result seems puzzling since it is more likely that the inclusion of BSSE effects would lead to a lengthening of the S−N bond distance. In fact, the present work finds that, at the B3LYP/6-311++G(d,p) level, the S−N bond lengths of the nitrogen-containing complexes of sulfur trioxide increase by no more than 0.04 Å when optimized including BSSE effects, and the $TMA-SO_3$ complex exhibits the smallest increase of only 0.024 Å. Even when the same level of theory is used that was employed by Choo et al.,[21] we find that the S−N bond of $TMA-SO_3$ increases by only 0.011 Å when BSSE effects are included in the optimization (1.942 Å with no BSSE correction compared to 1.953 Å with BSSE correction at the MPW1PW91/6-311+G(3df) level). On the basis of the present investigations, only small BSSE effects are obtained for the complexes, and hence the results reported in this work are not corrected for BSSE effects.

Atomic charges were determined by natural population analysis (NPA)[46] using the NBO 5.0 software package.[47] The charge transfer was computed as the amount of charge transferred from the oxygen- or nitrogen-containing donor molecule to sulfur trioxide in the intermolecular complex using the NPA charges.

All of the calculations were carried out on SGI O2, SGI Origin200, and Linux workstations at Illinois State University and on the IBM p690 supercomputer at the National Center for Supercomputing Applications.

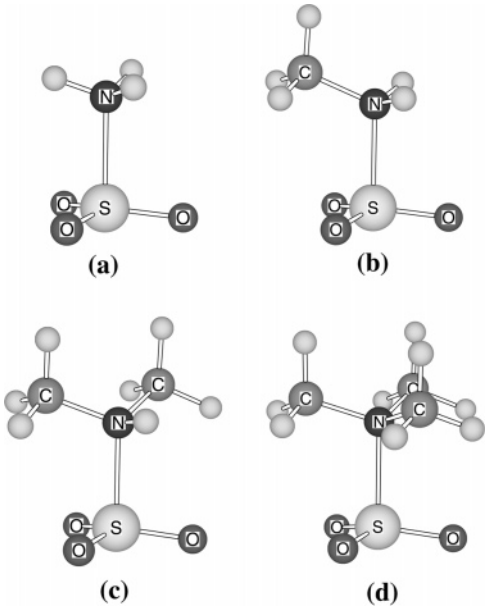

Figure 1. Optimized gas-phase geometries of (a) H_3N-SO_3, (b) $(CH_3)H_2N-SO_3$, (c) $(CH_3)_2HN-SO_3$, and (d) $(CH_3)_3N-SO_3$ determined at the B3LYP/6-31+G(d) level.

Results

1. Intermolecular Complexes of Sulfur Trioxide and Nitrogen-Containing Molecules. The optimized gas-phase structures of the complexes $(CH_3)_nH_{3-n}N-SO_3$ ($n = 0-3$) computed at the B3LYP/6-31+G(d) level are shown in Figure 1. Only small differences are observed in the geometries computed at the B3LYP/6-311++G(d,p) level of theory. The optimized condensed-phase structures are similar to those presented in Figure 1 and are not shown.

Selected geometrical parameters determined in the gas and condensed phases using the B3LYP/6-31+G(d) and B3LYP/6-311++G(d,p) levels of theory are presented in Table 1 along with available experimental data. The calculated gas-phase S−N bond distances of H_3N-SO_3 and TMA−SO_3 are too long by 0.14−0.17 Å compared to the experimental results. Similarly, the calculated condensed-phase S−N bond distances of all the complexes formed from nitrogen-containing donor molecules and SO_3 are too long by 0.10−0.12 Å compared to the experimental solid-state results. This overestimate of the calculated S−N bond distances may be partly due to electron correlation effects and partly due to the size of the basis sets employed in the present work. For example, calculations at the B3LYP/6-31+G(d) level yield a S−N distance of 2.100 Å for H_3N-SO_3 compared to 2.067 Å at the MP2/6-31+G(d) level, and, at the B3LYP/aug-cc-pV(T+d)Z level, the S−N distance is computed to be 2.049 Å.

The calculated gas- and condensed-phase average O−S−N angles of the nitrogen-containing complexes of sulfur trioxide are in good agreement with available experimental data, although they are, in all cases, slightly too small compared to the experimental results, exhibiting deviations of, at most, 2°. Leopold and co-workers noted a correlation between the S−N distances and the O−S−N bond angles in a variety of S−N donor−acceptor complexes.[13] These authors observed little variation in the O−S−N bond angle over a fairly large range of S−N distances. They were able to fit bond length and bond angle data to a relationship of the form

$$R(\mathrm{S-N}) = R_o + c \log[9 \cos^2 \alpha] \qquad (1)$$

where R(S−N) is the sulfur−nitrogen bond distance in angstroms, α is the O−S−N bond angle, $R_o = 1.621$ Å, and $c = -0.449$.[13] This empirical equation has its origins in Pauling's bond-length−bond-order relation.[48] The S−N bond distances computed in this work follow a similar trend; however, since the computational S−N bond distances are a little longer than the experimental ones, a value for R_o of about 1.69 Å provides a better fit to the computational results. The only exception to the bond-length−bond-angle correlation occurs for the TMA−SO_3 complex. Because of steric effects from the three methyl groups, the O−S−N angle is larger by about 1 degree than the value predicted by the fit.

Table 2 presents gas- and condensed-phase results for the binding energy, dipole moment, and charge transfer of the $(CH_3)_nH_{3-n}N-SO_3$ complexes. There is again only a small variation in these properties with respect to basis set. Furthermore, the calculated gas- and condensed-phase dipole moments are in excellent agreement with the available experimental data for H_3N-SO_3 and TMA−SO_3.

Figure 2 presents representative examples of trends in the properties of the $(CH_3)_nH_{3-n}N-SO_3$ complexes as methyl groups are added to the donor molecule. For the S−N bond lengths, the general trend in the gas-phase results is that the S−N distance decreases, with the exception of TMA−SO_3. Qualitatively, the gas-phase results are sensible because methyl groups are generally expected to act as electron-donating groups. An increase in the number of methyl groups leads to enhanced charge transfer and therefore shorter S−N bonds in the gas phase: an observed drop from H_3N-SO_3 to DMA−SO_3 of

TABLE 1: Selected Gas- and Condensed-Phase Bond Lengths (Å) and Angles (degrees) of $(CH_3)_nH_{3-n}N-SO_3$ ($n = 0-3$) along with Available Experimental Results.

	B3LYP/6-31+G(d)			B3LYP/6-311++G(d,p)			experiment		
	gas	solution	Δ[a]	gas	solution	Δ[a]	gas	solid	Δ[a]
H_3N-SO_3									
R(S−N)	2.100	1.895	−0.205	2.131	1.896	−0.235	1.957[c]	1.7714[d]	−0.186
∠O−S−N[b]	96.7	100.4	3.7	96.6	100.5	3.9	97.6[c]	102.46[d]	4.9
$(CH_3)H_2N-SO_3$									
R(S−N)	2.035	1.886	−0.149	2.055	1.890	−0.165		1.779[e]	
∠(O−S−N)[b]	97.6	100.9	3.3	97.5	100.8	3.3		102.4[e]	
$(CH_3)_2HN-SO_3$									
R(S−N)	2.028	1.908	−0.120	2.039	1.908	−0.131		1.790[f]	
∠(O−S−N)[b]	98.2	100.9	2.7	98.1	101.0	2.9		102.1[f]	
$(CH_3)_3N-SO_3$									
R(S−N)	2.050	1.946	−0.104	2.057	1.947	−0.110	1.912[g]	1.844[h]	−0.068
∠(O−S−N)[b]	98.6	101.0	2.4	98.5	100.9	2.4	100.1[g]	101.8[h]	1.7

[a] Δ is the difference between the condensed-phase and gas-phase values. [b] An average of the O−S−N angles is reported. [c] Ref 9. [d] Ref 10. [e] Ref 42. [f] Ref 43. [g] Ref 11. [h] Ref 12.

TABLE 2: Binding Energy (kcal/mol), Dipole Moment (Debye), and Charge Transfer in the Gas and Condensed Phases for $(CH_3)_nH_{3-n}N-SO_3$ ($n = 0-3$) along with Available Experimental Data

	B3LYP/6-31+G(d)			B3LYP/6-311++G(d,p)			experiment		
	gas	solution	Δ^a	gas	solution	Δ^a	gas	solid	Δ^a
H_3N-SO_3									
binding energy	17.78	34.84	17.06	16.86	33.81	16.95			
dipole moment	6.17	9.63	3.46	6.00	9.64	3.64	6.204[b]	9.6[c]	3.4
charge transfer	0.25	0.43	0.18	0.23	0.44	0.21			
$(CH_3)H_2N-SO_3$									
binding energy	23.18	39.99	16.81	22.54	38.26	15.72			
dipole moment	6.88	10.30	3.42	6.74	10.11	3.37			
charge transfer	0.30	0.45	0.15	0.29	0.45	0.16			
$(CH_3)_2HN-SO_3$									
binding energy	25.88	38.74	12.86	25.83	38.43	12.60			
dipole moment	7.12	10.40	3.28	7.00	10.14	3.14			
charge transfer	0.32	0.44	0.12	0.32	0.44	0.12			
$(CH_3)_3N-SO_3$									
binding energy	26.08	35.43	9.35	26.80	35.90	9.10			
dipole moment	7.11	10.39	3.28	6.99	10.09	3.10	7.111[d]		
charge transfer	0.32	0.43	0.11	0.32	0.43	0.11			

[a] Δ is the difference between the condensed-phase and gas-phase values. [b] Ref 4. [c] Ref 5. [d] Ref 1.

0.07−0.09 Å, depending on the basis set. The exception, TMA−SO_3, is probably due to increased steric effects from the three methyl groups as the S−N distance decreases. The condensed-phase behavior of the S−N bond distance is quite different than the gas-phase behavior. In the condensed phase, as the number of methyl groups of the donor molecule increases, the S−N distance generally increases. Steric effects dominate the condensed-phase results since the S−N distance is already much shorter in the condensed phase than it is in the gas phase. An increase in the number of methyl groups of the donor molecule in the condensed phase increases the steric repulsion and leads to a slight increase of 0.05 Å in S−N bond distance from MA−SO_3 to TMA−SO_3.

While the S−N distance shows a significant variation as the number of methyl groups on the nitrogen-containing donor molecule is increased, other geometrical parameters show little change. For example, the average O−S−N angle increases only slightly as the number of methyl groups increases. The change in the O−S−N angle is less than 2° in the gas phase and less than 1° in the condensed phase.

As methyl groups are added to the nitrogen-containing donor molecule, the gas-phase binding energies and dipole moments show a significant enhancement. The binding energy grows by more than 8 kcal/mol, and the dipole moment grows by nearly 1 D from H_3N-SO_3 to TMA−SO_3. These changes correlate directly with the shorter S−N bond distances observed as methyl groups are added. In the condensed phase, on the other hand, the binding energy and dipole moments show smaller variation as methyl groups are added to the donor molecule. From H_3N-SO_3 to MA−SO_3, the condensed-phase binding energy increases by 4−5 kcal/mol, and the dipole moment increases by 0.5−0.6 D. When the number of methyl groups is increased further, the values of the binding energy and dipole moment level off and then decrease slightly from DMA−SO_3 to TMA−SO_3. This is likely a consequence of the increased steric repulsion in the DMA−SO_3 and TMA−SO_3 complexes.

The gas-phase charge transfer calculated using NPA exhibits a moderate gain of 0.07−0.09 as the number of methyl groups increases. Conversely, in the condensed phase, the charge transfer remains nearly steady, regardless of the number of methyl groups of the donor.

As expected from previous experimental and computational studies, the intermolecular complexes formed between the nitrogen-containing molecules $(CH_3)_nH_{3-n}N$ and SO_3 display significant differences in geometries and properties in the gas and condensed phases, which are also illustrated in Figure 2. The largest gas/condensed-phase alterations are observed in S−N distances, binding energies, dipole moments, and charge transfer. The S−N distance decreases substantially in the condensed phase, by over 0.2 Å for H_3N-SO_3 and by about 0.1 Å for TMA−SO_3, with intermediate values for the other complexes. These changes are in good agreement with the experimentally observed gas/solid differences for H_3N-SO_3 and TMA−SO_3. In addition, the binding energies increase by 9−17 kcal/mol in the condensed phase, with the largest change observed for H_3N-SO_3. Because of the ability of the condensed phase to support larger charge separation, the dipole moments jump by more than 3 D in the condensed phase. A corresponding enhancement of the charge transfer of around 0.1−0.2 is also observed in the condensed phase.

Since the results suggest that the observed increases in the binding energy, dipole moment, and charge transfer as well as the significant drop in S−N distance in the condensed phase are due to the ability of the condensed-phase medium to support higher charge separation, the natural atomic charges calculated using NPA have been examined. Table 3 presents gas- and condensed-phase results for H_3N-SO_3 as well as H_2O-SO_3 (which will be discussed in the next section). Striking differences of around 0.2 in the total charge of the oxygen atoms of SO_3 and the total charge of the hydrogen atoms of NH_3 are observed between the gas and condensed phases. Conversely, the charges of the sulfur and nitrogen atoms remain nearly constant in the gas and condensed phases. The overall result is that the condensed phase supports a higher charge distribution on the extremities of the molecule. The bulk of the enhanced charge transfer in the solution phase is pulled from the hydrogen atoms of NH_3 and redistributed to the oxygen atoms of SO_3, leading to a larger condensed-phase charge separation. The other nitrogen-containing complexes exhibit similar, though slightly more modest, gas/condensed-phase charge separation.

2. Intermolecular Complexes of Sulfur Trioxide and Oxygen-Containing Molecules. The optimized gas-phase structures of the donor−acceptor complexes $(CH_3)_mH_{2-m}O-SO_3$ ($m = 0-2$) computed at the B3LYP/6-31+G(d) level are shown in Figure 3. The condensed-phase structures are similar to those presented in Figure 3 and are not shown. In general, only small differences are observed in the geometries computed at the B3LYP/6-311++G(d,p) level of theory and those obtained at

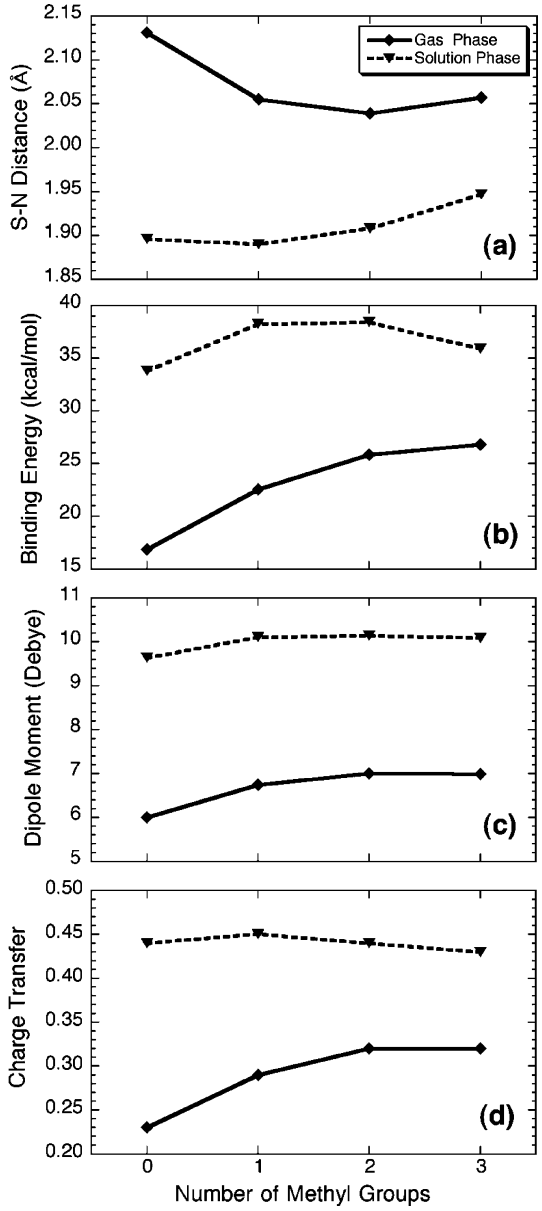

Figure 2. Gas- and solution-phase (a) S−N bond distances, (b) binding energies, (c) dipole moments, and (d) charge transfer as a function of the number of methyl groups of the nitrogen-containing donor for $(CH_3)_nH_{3-n}N-SO_3$ complexes computed at the B3LYP/6-311++G(d,p) level.

the B3LYP/6-31+G(d) level. The one minor exception occurs for H_2O-SO_3, with a structure at all but one level of theory that has an orientation in which the O−H bonds of H_2O are eclipsed relative to the S−O bonds of SO_3. However, the gas-phase structure of H_2O-SO_3 at the B3LYP/6-311++G(d,p) level has an orientation in which the O−H bonds are staggered relative to the S−O bonds. This anomalous result is a consequence of the very low barrier to rotation about the intermolecular axis. In previous work, the barrier for rotation about the intermolecular axis of H_2O-SO_3 was computed to be only 0.1 kcal/mol at the MP2/6-311++G(2df,2pd) level of theory.[34]

Table 4 presents selected geometrical parameters of the $(CH_3)_mH_{2-m}O-SO_3$ complexes determined in the gas and condensed phases using the B3LYP/6-31+G(d) and B3LYP/6-311++G(d,p) levels of theory along with available experimental results. For H_2O-SO_3 in the gas phase, the computed values of the S−O_d distance and the average O_a−S−O_d angle

TABLE 3: Natural Atomic Charges of H_3N-SO_3 and H_2O-SO_3

	B3LYP/6-31+G(d)			B3LYP/6-311++G(d,p)		
	gas	solution	Δ[a]	gas	solution	Δ[a]
H_3N-SO_3						
S	2.44	2.48	0.04	2.37	2.39	0.02
O total[b]	−2.69	−2.91	−0.22	−2.60	−2.83	−0.23
N	−1.10	−1.08	0.02	−0.98	−0.94	0.04
H total[c]	1.35	1.51	0.16	1.22	1.38	0.16
H_2O-SO_3						
S	2.42	2.46	0.04	2.35	2.39	0.04
O_a total[b]	−2.49	−2.66	−0.17	−2.41	−2.56	−0.15
O_d	−0.98	−0.97	0.01	−0.92	−0.92	0.00
H total[c]	1.05	1.17	0.12	0.98	1.09	0.11

[a] Δ is the difference between the condensed-phase and gas-phase values. [b] The reported value is the sum of the natural atomic charges of the three oxygen atoms of SO_3. [c] The reported value is the sum of the natural atomic charges of the three hydrogen atoms of NH_3 or the two hydrogen atoms of H_2O.

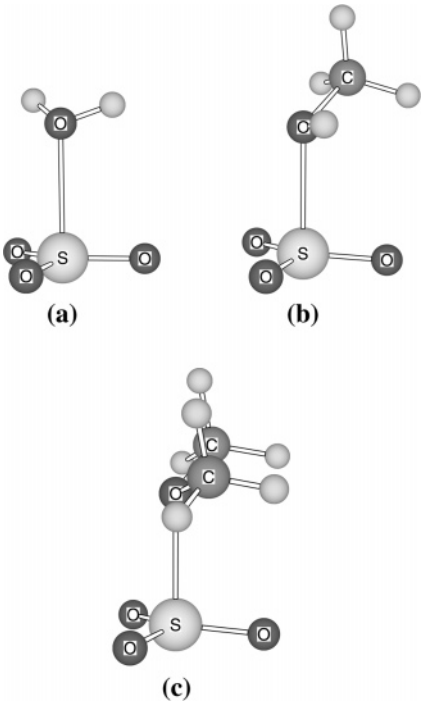

Figure 3. Optimized gas-phase geometries of (a) H_2O-SO_3, (b) $CH_3-OH-SO_3$, and (c) $(CH_3)_2O-SO_3$ determined at the B3LYP/6-31+G(d) level.

are in excellent agreement with the experimental gas-phase results. Deviations in the S−O_d bond length are less than 0.04 Å, and those in the O_a−S−O_d bond angle are less than 0.5°. In Table 5, the calculated gas- and condensed-phase results for the binding energies, dipole moments, and charge transfer are listed for the $(CH_3)_mH_{2-m}O-SO_3$ complexes. The geometries and other properties show little variation as a function of basis set size for these complexes.

The gas-phase oxygen-containing complexes of sulfur trioxide have S−O_d bonds that are 0.2−0.3 Å longer than the corresponding S−N bonds of the nitrogen-containing complexes, and the condensed-phase S−O_d bonds are about 0.1−0.2 Å longer than the corresponding S−N bonds. In addition, the binding energies of the oxygen-containing complexes are significantly lower than those of the corresponding nitrogen-containing complexes, by about 10−15 kcal/mol in the gas phase and 20−25 kcal/mol in the condensed phase. These differences are expected for oxygen- and nitrogen-containing systems on the basis of electronegativities. The larger electronegativity of

TABLE 4: Selected Gas- and Condensed-Phase Bond Lengths (Å) and Angles (degrees) of $(CH_3)_mH_{2-m}O-SO_3$ ($m = 0-2$) along with Available Experimental Results

	B3LYP/6-31+G(d)			B3LYP/6-311++G(d,p)			expt
	gas	solution	Δ^a	gas	solution	Δ^a	gas
H_2O-SO_3							
$R(S-O_d)^b$	2.394	2.093	−0.301	2.413	2.144	−0.267	2.432[d]
$\angle O_a-S-O_d{}^c$	93.1	96.7	3.6	93.0	96.2	3.0	92.6[d]
CH_3OH-SO_3							
$R(S-O_d)^b$	2.255	1.987	−0.268	2.275	2.023	−0.252	
$\angle(O_a-S-O_d)^c$	94.3	97.8	3.5	94.2	97.5	3.3	
$(CH_3)_2O-SO_3$							
$R(S-O_d)^b$	2.212	2.017	−0.195	2.222	2.043	−0.179	
$\angle(O_a-S-O_d)^c$	95.1	97.8	2.7	94.9	97.4	2.5	

[a] Δ is the difference between the condensed-phase and gas-phase values. [b] Atom O_d corresponds to the oxygen atom of the donor molecule, $(CH_3)_mH_{2-m}O$ ($m = 0-2$). [c] Atom O_a refers to any of the three oxygen atoms of the acceptor molecule SO_3. The average O_a-S-O_d angle is reported. [d] Ref 25.

TABLE 5: Binding Energy (kcal/mol), Dipole Moment (Debye), and Charge Transfer in the Gas and Condensed Phases for $(CH_3)_mH_{2-m}O-SO_3$ ($m = 0-2$)

	B3LYP/6-31+G(d)			B3LYP/6-311++G(d,p)		
	gas	solution	Δ^a	gas	solution	Δ^a
H_2O-SO_3						
binding energy	7.80	13.55	5.76	7.60	13.17	2.15
dipole moment	3.46	6.23	2.77	3.55	5.92	2.29
charge transfer	0.07	0.20	0.13	0.06	0.17	0.11
CH_3OH-SO_3						
binding energy	10.24	17.23	6.99	10.40	16.74	6.34
dipole moment	4.39	7.55	3.16	4.29	7.27	2.98
charge transfer	0.12	0.25	0.13	0.11	0.24	0.13
$(CH_3)_2O-SO_3$						
binding energy	11.01	15.20	4.19	11.79	15.55	3.76
dipole moment	4.72	7.55	2.83	4.63	7.28	2.65
charge transfer	0.14	0.24	0.10	0.13	0.23	0.10

[a] Δ is the difference between the condensed-phase and gas-phase values.

oxygen leads to less electron transfer from the oxygen to the sulfur and thus weaker bonds and longer bond lengths. The trends in bond lengths and binding energies for oxygen- and nitrogen-containing complexes are confirmed by the charge transfer calculated using NPA, which is about 0.2−0.3 lower for the oxygen-containing complexes.

As was the case for the nitrogen-containing complexes, a correlation between the calculated $S-O_d$ bond distances and O_a-S-O_d bond angles of the oxygen-containing complexes is observed. Using eq 1, the computational $S-O_d$ bond distances and O_a-S-O_d bond angles fall on nearly the same trend line as the computational S−N bond distances and O−S−N bond angles of the nitrogen-containing complexes. Leopold and co-workers also found that the B−N distances and H−B−N or F−B−N bond angles of donor−acceptor complexes containing BH_3 or BF_3 followed a similar trend to the bond-distance/bond-angle correlations of the S−N donor−acceptor complexes.[13]

Illustrative examples of trends in selected properties of the $(CH_3)_mH_{2-m}O-SO_3$ complexes as methyl groups are added to the donor molecule are shown in Figure 4. The calculated gas-phase $S-O_d$ bond distance decreases by 0.18−0.19 Å as methyl groups are added to the donor molecule. This change is more than double that observed for the S−N distance of the nitrogen-containing complexes and is in accord with the viewpoint of the methyl groups acting as electron donors. The behavior of the $S-O_d$ distance in the condensed phase and the behavior of other geometrical parameters in the gas and condensed phases are consistent with the behaviors observed for the nitrogen-containing complexes. The condensed-phase $S-O_d$ distance drops when one methyl group is added but increases with the addition of a second methyl group because of steric effects that arise as a result of the much shorter condensed-phase $S-O_d$ bond distance. Other geometrical parameters show smaller

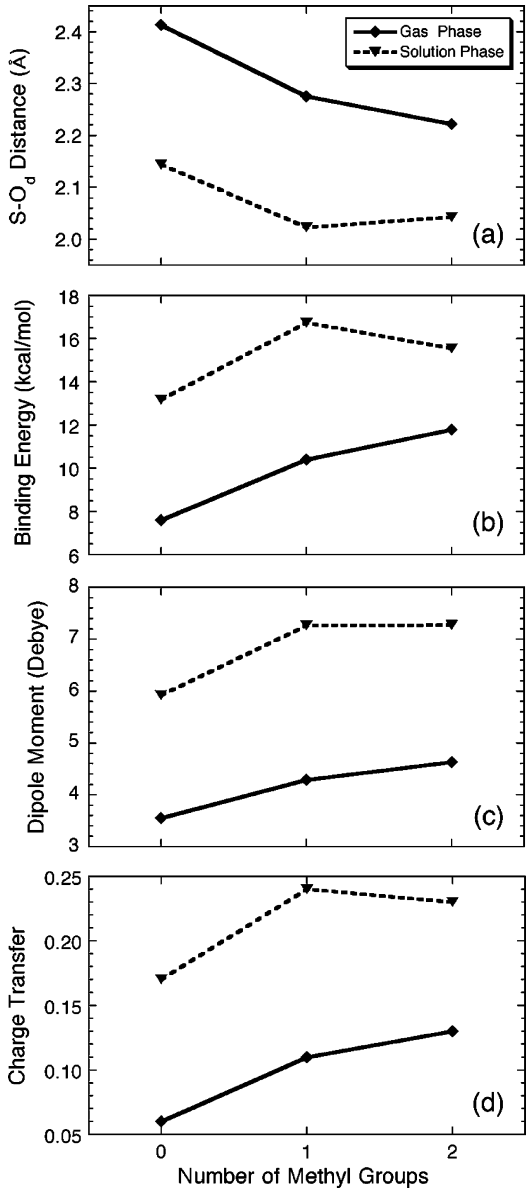

Figure 4. Gas- and solution-phase (a) $S-O_d$ bond distances, (b) binding energies, (c) dipole moments, and (d) charge transfer as a function of the number of methyl groups of the oxygen-containing donor for $(CH_3)_mH_{2-m}O-SO_3$ complexes computed at the B3LYP/6-311++G-(d,p) level.

changes as the number of methyl groups on the donor is increased. For example, in both the gas and condensed phases, the average O_a-S-O_d angle grows by a modest 1−2° as methyl groups are added to the donor molecule.

The behavior of the binding energy, dipole moment, and charge transfer as a function of the number of methyl groups is similar for the oxygen- and nitrogen-containing complexes. As the number of methyl groups increases, the gas-phase binding energies of the oxygen-containing complexes increase by 3−4 kcal/mol, and the dipole moments increase by about 1 D, which correlate to decreases in the $S-O_d$ bond distance. Conversely, in the condensed phase, the binding energy and dipole moments grow with the addition of one methyl group to the oxygen-containing donor and then decrease or level off as the second methyl group is added, a consequence of the enhanced steric repulsion. In the gas phase, the charge transfer slightly increases by 0.07 as methyl groups are added; however, in the condensed phase, the charge transfer behaves in a fashion similar to the dipole moment, with a small increase for one methyl group and then a slight decrease when the second methyl group is added.

Like the $(CH_3)_nH_{3-n}N-SO_3$ complexes, the $(CH_3)_mH_{2-m}O-SO_3$ complexes show significant differences in geometries and properties in the gas phase and in the condensed phase, as also illustrated in Figure 4. Unlike the nitrogen-containing complexes H_3N-SO_3 and $TMA-SO_3$, no experimental data exists for the gas/condensed-phase properties of the oxygen-containing complexes. Thus, the computational results presented in this work provide information about a new class of donor−acceptor complexes that should be accessible by experiment and that exhibit large gas/condensed-phase deviations.

For the oxygen-containing complexes, the $S-O_d$ bond distance and the dipole moments show the largest gas/condensed-phase changes. The condensed-phase $S-O_d$ distance decreases by about 0.3 Å for H_3O-SO_3 and by about 0.2 Å for $(CH_3)_2O-SO_3$. The gas/condensed-phase differences in the $S-O_d$ distance are about 0.1 Å larger than the differences observed in the S−N bond distances of the nitrogen-containing complexes. In addition, the dipole moments of the oxygen-containing complexes exhibit a gain of about 3 D in the condensed phase, a similar change to that observed for the nitrogen-containing complexes.

More moderate gas/condensed-phase deviations are also observed in other properties of the oxygen-containing complexes. The condensed-phase binding energies are 2−7 kcal/mol higher than the gas-phase binding energies, a smaller difference than that observed for the nitrogen-containing complexes. Finally, the condensed-phase charge transfer of the oxygen-containing complexes is higher by about 0.1 than the gas-phase charge transfer, in accord with the results determined for the nitrogen-containing complexes.

The enhanced charge separation in the condensed phase is also evident for the oxygen-containing complexes, as illustrated in Table 3 for H_2O-SO_3 (the results for other oxygen-containing complexes are similar). In accord with the results found for the nitrogen-containing complexes, the charges of the sulfur atom and the oxygen atom of H_2O remain nearly constant in the gas and condensed phases. However, the oxygen atoms of SO_3 become significantly more negative, and the hydrogen atoms of H_2O become much more positive in the condensed phase. These results support the notions of stabilization of higher charge density on the extremities of the molecule and enhanced condensed-phase charge separation.

Conclusions

Systematic computational studies of the gas- and condensed-phase behavior of nitrogen- and oxygen-containing donor−acceptor complexes of sulfur trioxide have been presented for the first time. Gas-phase and condensed-phase PCM continuum solvation results obtained using density functional theory are in excellent agreement with available experimental data. Furthermore, the gas/condensed-phase behavior of two nitrogen-containing complexes, $(CH_3)H_2N-SO_3$ and $(CH_3)_2HN-SO_3$, has been explored for the first time, and two new oxygen-containing complexes never before studied, CH_3OH-SO_3 and $(CH_3)_2O-SO_3$, have been characterized.

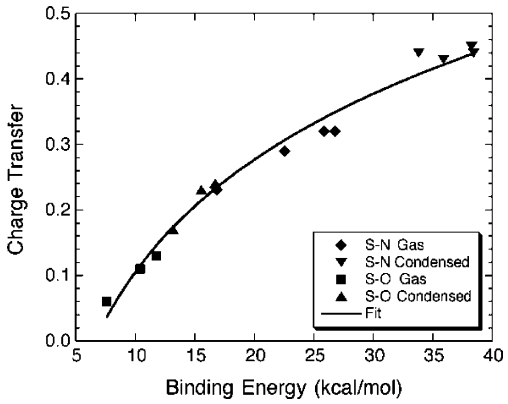

Figure 5. Correlation between charge transfer and binding energy for nitrogen- and oxygen-containing complexes of sulfur trioxide computed at the B3LYP/6-311++G(d,p) level.

In previous work, Frenking and co-workers employed NPA to determine the charge transfer in donor−acceptor complexes for a wide variety of acceptors, including SO_2, BH_3, BF_3, BCl_3, and $AlCl_3$.[18] For this large range of complexes with varying amounts of covalent bonding character, they found no correlation between charge transfer and binding energy. In contrast, a strong correlation between charge transfer and binding energy is observed in the gas and condensed phases for both the nitrogen- and oxygen-containing complexes of sulfur trioxide. Figure 5 illustrates the logarithmic correlation between binding energy and charge transfer for calculations performed in the gas and condensed phases using the B3LYP/6-311++G(d,p) level of theory. Results determined at the B3LYP/6-31+G(d) level show a similar correlation. The strong correlation between charge transfer and binding energy for the sulfur trioxide complexes emphasizes the important role that charge transfer plays in determining the bonding in these systems.

All the donor−acceptor complexes investigated in this work exhibit significant gas/condensed-phase changes in geometrical parameters and other properties. Each complex displays a sizable decrease in intermolecular bond distance and large increases in binding energy, dipole moment, and charge transfer from the gas phase to the condensed phase. The origin of these effects lies in the enhanced stabilization of the charge separation in the condensed-phase medium compared to that in the gas phase, as illustrated through NPA results. The NPA results also show that significant amounts of charge shift from the hydrogen atoms of the nitrogen- or oxygen-containing donor to the oxygen atoms of sulfur trioxide, enhancing the charge density on the extremities of the complexes.

Both sets of compounds show comparable behavior in the gas and condensed phases as methyl groups are added to the donor molecule. In the gas phase, the added methyl groups act as electron-donating groups and lead to shorter intermolecular bond distances and larger binding energies, dipole moments, and charge transfer. In the condensed phase, the intermolecular distance initially drops when one methyl group is added. However, because the intermolecular distance is significantly

shorter in the condensed phase, further addition of methyl groups leads to an increase in intermolecular bond distance as a result of enhanced steric repulsion. Changes in other condensed-phase properties correlate with the changes in the intermolecular distance.

The two nitrogen compounds never previously studied in both the gas and condensed phases, $MA-SO_3$ and $DMA-SO_3$, exhibit gas/condensed-phase changes that are generally intermediate between those of H_3N-SO_3 and $TMA-SO_3$, and hence their gas/condensed-phase behavior should fall within the realm of possible experimental observation. The predicted behavior of the new oxygen-containing compounds probed in this work is particularly intriguing. The gas/condensed-phase changes in the intermolecular $S-O_d$ bond distances of the oxygen-containing complexes are predicted to be even larger than those of the S−N bond in the nitrogen-containing complexes. Thus, synthesis and experimental detection of the oxygen-containing complexes CH_3OH-SO_3 and $(CH_3)_2O-SO_3$ should provide additional avenues for exploration of gas/condensed-phase behavior in a new class of donor−acceptor complexes.

Acknowledgment. The authors thank the reviewers for helpful suggestions. This research was partially supported by Research Corporation through Cottrell College Science Award No. CC-6282. Partial support of this work through an award of supercomputer time at the National Center for Supercomputing Applications is also acknowledged.

References and Notes

(1) Leopold, K. R.; Canagaratna, M.; Phillips, J. A. *Acc. Chem. Res.* **1996**, *30*, 57.

(2) Dvorak, M. A.; Ford, R. S.; Suenram, R. D.; Lovas, F. J.; Leopold, K. R. *J. Am. Chem. Soc.* **1992**, *114*, 108.

(3) (a) Hoard, J. L.; Owen, T. B.; Buzzell, A.; Salmon, O. N. *Acta Crystallogr.* **1950**, *3*, 130. (b) Swanson, B.; Shriver, D. F.; Ibers, J. A. *Inorg. Chem.* **1969**, *8*, 2183.

(4) Reeve, S. W.; Burns, W. A.; Lovas, F. J.; Suernam, R. D.; Leopold, K. R. *J. Phys. Chem.* **1993**, *97*, 10630.

(5) Burns, W. A.; Leopold, K. R. *J. Am. Chem. Soc.* **1993**, *115*, 11622.

(6) Phillips, J. A.; Britton, D.; Leopold, K. R. *J. Chem. Cryst.* **1996**, *26*, 533.

(7) Oh, J. J.; Hillig, K. W., II; Kuczkowski, R. L. *J. Phys. Chem.* **1991**, *95*, 7211.

(8) Oh, J. J.; LaBarge, M. S.; Matos, J.; Kampf, J. W.; Hillig, K. W., II; Kuczkowski, R. L. *J. Am. Chem. Soc.* **1991**, *113*, 4732.

(9) Canagaratna, M.; Phillips, J. A.; Goodfriend, H.; Leopold, K. R. *J. Am. Chem. Soc.* **1996**, *118*, 5290.

(10) (a) Kanda, F. A.; King, A. J. *J. Am. Chem. Soc.* **1951**, *73*, 2315. (b) Sass, R. L. *Acta Crystallogr.* **1960**, *13*, 320. (c) Bats, J. W.; Coppens, P.; Koetzle, T. F. *Acta Crystallogr.* **1977**, *B33*, 37.

(11) Fiacco, D. L.; Toro, A.; Leopold, K. R. *Inorg. Chem.* **2000**, *39*, 37.

(12) Morris, A. J.; Kennard, C. H. L.; Hall, J. R.; Smith, G.; White, A. H. *Acta Crystallogr.* **1983**, *C39*, 81.

(13) Burns, W. A.; Phillips, J. A.; Canagaratna, M.; Goodfriend, H.; Leopold, K. R. *J. Phys. Chem. A* **1999**, *103*, 7445.

(14) Canagaratna, M.; Ott, M. E.; Leopold, K. R. *Chem. Phys. Lett.* **1997**, *281*, 63.

(15) Coppens, P.; Guru Row, T. N.; Leung, P.; Stevens, E. D.; Becker, P. J.; Yang, Y. W. *Acta Crystallogr.* **1979**, *A35*, 63.

(16) Wong, M. W.; Wiberg, K. B.; Frisch, M. J. *J. Am. Chem. Soc.* **1992**, *114*, 523.

(17) Cioslowski, J.; Martinov, M. *J. Chem. Phys.* **1995**, *103*, 4967.

(18) Jonas, V.; Frenking, G.; Reetz, M. T. *J. Am. Chem. Soc.* **1994**, *116*, 8741.

(19) Merino, G.; Bakhmutov, V. L.; Vela, A. *J. Phys. Chem. A* **2002**, *106*, 8491.

(20) Dillen, J.; Verhoeven, P. *J. Phys. Chem. A* **2003**, *107*, 2570.

(21) Choo, J.; Kim, S.; Kwon, Y. *J. Mol. Struct. (THEOCHEM)* **2002**, *594*, 147.

(22) Tso, T.-L.; Lee, E. K. C. *J. Phys. Chem.* **1984**, *88*, 2776.

(23) Bondybey, V. E.; English, J. H. *J. Mol. Spectrosc.* **1985**, *109*, 221.

(24) Shriver, L.; Carrere, D.; Schriver, A.; Jaeger, K. *Chem. Phys. Lett.* **1991**, *181*, 505.

(25) Phillips, J. A.; Canagaratna, M.; Goodfriend, H.; Leopold, K. R. *J. Phys. Chem.* **1995**, *99*, 501.

(26) Holland, P. M.; Castleman, A. W., Jr. *Chem. Phys. Lett.* **1978**, *56*, 511.

(27) Chen, T. S.; Plummer, P. L. M. *J. Am. Chem. Soc.* **1985**, *89*, 3689.

(28) Hofmann, M.; Schleyer, P. v. R. *J. Am. Chem. Soc.* **1994**, *116*, 4947.

(29) Morokuma, K.; Muguruma, C. *J. Am. Chem. Soc.* **1994**, *116*, 10316.

(30) Meijer, E. J.; Sprik, M. *J. Phys. Chem. A* **1998**, *102*, 2893.

(31) Larson, L. J.; Kuno, M.; Tao, F.-M. *J. Chem. Phys.* **2000**, *112*, 8830.

(32) Loerting, T.; Liedl, K. R. *Proc. Natl. Acad. Sci. U.S.A.* **2000**, *97*, 8874.

(33) Loerting, T.; Liedl, K. R. *J. Phys. Chem. A* **2001**, *105*, 5137.

(34) Standard, J. M.; Buckner, I. S.; Pulsifer, D. H. *J. Mol. Struct. (THEOCHEM)* **2004**, *673*, 1.

(35) Lovejoy, E. R.; Hanson, D. R. *J. Phys. Chem.* **1996**, *100*, 4459.

(36) Douglas, J. E.; Kenyon, G. L.; Kollman, P. A. *Chem. Phys. Lett.* **1978**, *57*, 553.

(37) Hickling, S. J.; Wooley, R. G. *Chem. Phys. Lett.* **1990**, *166*, 43.

(38) Mo, Y.; Gao, J. *J. Phys. Chem. A* **2001**, *105*, 6530.

(39) Hunt, S. W.; Brauer, C. S.; Craddock, M. B.; Higgins, K. J.; Nienow, A. M.; Leopold, K. R. *Chem. Phys.* **2004**, *305*, 155.

(40) Larson, L. J.; Tao, F.-M. *J. Phys. Chem. A* **2001**, *105*, 4344.

(41) Pawlowski, P.; Okimoto, S. R.; Tao, F.-M. *J. Phys. Chem. A* **2003**, *107*, 5327.

(42) Morris, A. J.; Kennard, C. H. L.; Hall, J. R.; Smith, G. *Inorg. Chim. Acta* **1982**, *62*, 247.

(43) Morris, A. J.; Kennard, C. H. L.; Hall, J. R. *Acta Crystallogr.* **1983**, *C39*, 1236.

(44) Frisch, M. J.; Trucks, G. W.; Schlegel, H. B.; Scuseria, G. E.; Robb, M. A.; Cheeseman, J. R.; Zakrzewski, V. G.; Montgomery, J. A., Jr.; Stratmann, R. E.; Burant, J. C.; Dapprich, S.; Millam, J. M.; Daniels, A. D.; Kudin, K. N.; Strain, M. C.; Farkas, O.; Tomasi, J.; Barone, V.; Cossi, M.; Cammi, R.; Mennucci, B.; Pomelli, C.; Adamo, C.; Clifford, S.; Ochterski, J.; Petersson, G. A.; Ayala, P. Y.; Cui, Q.; Morokuma, K.; Malick, D. K.; Rabuck, A. D.; Ragavachari, K.; Foresman, J. B.; Cioslowski, J.; Ortiz, J. V.; Baboul, A. G.; Stefanov, B. B.; Liu, G.; Liashenko, A.; Piskorz, P.; Komaromi, I.; Gomperts, R.; Martin, R. L.; Fox, D. J.; Keith, T.; Al-Laham, M. A.; Peng, C. Y.; Nanayakkara, A.; Gonzalez, C.; Challacombe, M.; Gill, P. M. W.; Johnson, B. G.; Chen, W.; Wong, M. W.; Andres, J. L.; Head-Gordon, M.; Replogle, E. S.; Pople, J. A. *Gaussian 98*, revision A.7; Gaussian, Inc.: Pittsburgh, PA, 1998.

(45) Frisch, M. J.; Trucks, G. W.; Schlegel, H. B.; Scuseria, G. E.; Robb, M. A.; Cheeseman, J. R.; Montgomery, J. A., Jr.; Vreven, T.; Kudin, K. N.; Burant, J. C.; Millam, J. M.; Iyengar, S. S.; Tomasi, J.; Barone, V.; Mennucci, B.; Cossi, M.; Scalmani, G.; Rega, N.; Petersson, G. A.; Nakatsuji, H.; Hada, M.; Ehara, M.; Toyota, K.; Fukuda, R.; Hasegawa, J.; Ishida, M.; Nakajima, T.; Honda, Y.; Kitao, O.; Nakai, H.; Klene, M.; Li, X.; Knox, J. E.; Hratchian, H. P.; Cross, J. B.; Bakken, V.; Adamo, C.; Jaramillo, J.; Gomperts, R.; Stratmann, R. E.; Yazyev, O.; Austin, A. J.; Cammi, R.; Pomelli, C.; Ochterski, J. W.; Ayala, P. Y.; Morokuma, K.; Voth, G. A.; Salvador, P.; Dannenberg, J. J.; Zakrzewski, V. G.; Dapprich, S.; Daniels, A. D.; Strain, M. C.; Farkas, O.; Malick, D. K.; Rabuck, A. D.; Raghavachari, K.; Foresman, J. B.; Ortiz, J. V.; Cui, Q.; Baboul, A. G.; Clifford, S.; Cioslowski, J.; Stefanov, B. B.; Liu, G.; Liashenko, A.; Piskorz, P.; Komaromi, I.; Martin, R. L.; Fox, D. J.; Keith, T.; Al-Laham, M. A.; Peng, C. Y.; Nanayakkara, A.; Challacombe, M.; Gill, P. M. W.; Johnson, B.; Chen, W.; Wong, M. W.; Gonzalez, C.; Pople, J. A. *Gaussian 03*, revision C.02, Gaussian, Inc.: Wallingford, CT, 2004.

(46) Reed, A. E.; Weinstock, R. B.; Weinhold, F. *J. Chem. Phys.* **1985**, *83*, 735.

(47) Glendening, E. D.; Badenhoop, J. K.; Reed, A. E.; Carpenter, J. E.; Bohmann, J. A.; Morales, C. M.; Weinhold, F. *NBO 5.0*; Theoretical Chemistry Institute, University of Wisconsin: Madison, WI, 2001.

(48) Pauling, L. *J. Am. Chem. Soc.* **1947**, *69*, 542.